
Neural Subgraph Matching

Rex Ying[†] Zhaoyu Lou[†] Jiaxuan You[†] Chengtao Wen[‡] Arquimedes Canedo[‡]
 Jure Leskovec[†]

[†]Department of Computer Science, Stanford University
 {rexy, zlou, jiaxuan, jure}@cs.stanford.edu

[‡]Siemens Corporate Technology
 {chengtao.wen, arquimedes.canedo}@siemens.com

Abstract

Subgraph matching is the problem of determining the presence and location(s) of a given query graph in a large target graph. Despite being an NP-complete problem, the subgraph matching problem is crucial in domains ranging from network science and database systems to biochemistry and cognitive science. However, existing techniques based on combinatorial matching and integer programming cannot handle matching problems with both large target and query graphs. Here we propose NeuroMatch, an accurate, efficient, and robust neural approach to subgraph matching. NeuroMatch decomposes query and target graphs into small subgraphs and embeds them using graph neural networks. Trained to capture geometric constraints corresponding to subgraph relations, NeuroMatch then efficiently performs subgraph matching directly in the embedding space. Experiments demonstrate NeuroMatch is 100x faster than existing combinatorial approaches and 18% more accurate than existing approximate subgraph matching methods.

1. Introduction

Given a query graph, the problem of subgraph isomorphism matching is to identify a subgraph of a large target graph that is isomorphic to the query graph. If the graphs include node and edge features, both the topology as well as the features should be matched.

Subgraph matching is a crucial problem in many biology, social network and knowledge graph applications [13, 21, 34, 9]. For example, in social networks and biomedical network science, researchers investigate important subgraphs by counting them in a given network [2]. In knowledge graphs, common substructures are extracted by querying them in the larger target graph [13, 20].

Traditional approaches make use of combinatorial search algorithms [8, 12, 26, ?]. However, they do not scale to large problem sizes due to the NP-complete nature of the problem. Existing efforts to scale up subgraph isomorphism [25] make use of expensive pre-processing to store locations of many small 2-4 node components, and decompose the queries into these components. Although this allows matching to scale to large target graphs, the size of the query cannot scale to more than a few tens of nodes before decomposing the query becomes a hard problem by itself.

Here we propose NeuroMatch, the first neural approach for subgraph matching that can scale to both large query G_Q (up to 500 nodes) and large target graphs G_T (up to 50,000 nodes). The core of NeuroMatch is to decompose the target G_T as well as the query G_Q into many small overlapping graphs and use a Graph Neural Network (GNN) to embed the individual graphs such that we can then quickly determine whether one graph is a subgraph of another.

Our approach works in two stages, an embedding stage and a query stage. At the embedding stage, we decompose the target graph G_T into many sub-networks G_u : For every node $u \in G_T$ we extract a k -hop sub-network G_u around u and use a GNN to obtain an embedding for u . At the query stage,

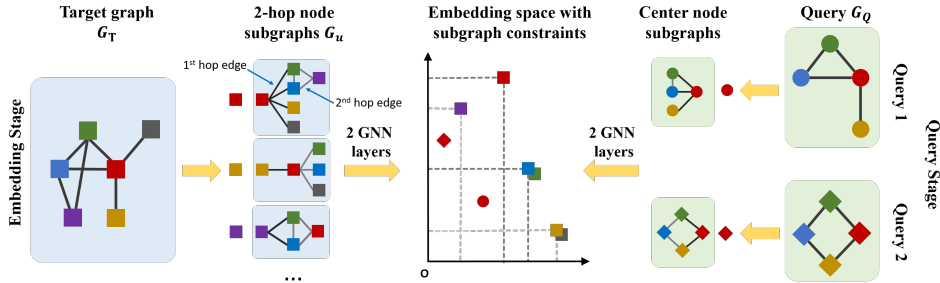


Figure 1: **Overview of NeuroMatch.** We decompose target graph G_T by extracting k -hop subgraph G_u centered at every node u . We then use a GNN to embed each G_u (left). We refer to u as the center node of G_u . We train the GNN to reflect the subgraph relationships: If G_v is a subgraph of G_u , then node v should be embedded to the lower-left of u . For example, since the 2-hop graph of the violet node is a subgraph of the 2-hop graph of the red node, the embedding of the violet square is to the lower-left of the red square node. At the query stage, we decompose the query G_Q by picking its center node q and embed it. From the embedding itself we can quickly determine that Query 1 is a subgraph of the red, blue, and green nodes because its embedding is to the lower-left of them. Similarly, Query 2 is a subgraph of the purple and red nodes and is thus positioned to the lower-left of both nodes. Notice NeuroMatch avoids expensive combinatorial matching of subgraphs.

we create k -hop sub-network G_q around a node q in the query graph G_Q . We embed each G_q using a GNN centered at node q . We then compare embeddings of nodes q and u (i.e., graphs G_q and G_u) and use a voting mechanism to determine whether G_Q is a subgraph of G_T .

The key insight that makes NeuroMatch work is to define an embedding space where subgraph relationships are preserved. We observe that subgraph relationships induce a partial ordering over subgraphs. This observation inspires the use of geometric set embeddings such as order embeddings [19] and box embeddings [28], which induce a partial ordering on embeddings with geometric shapes. By ensuring that the partial ordering on embeddings reflects the ordering on subgraphs, we equip our model with a powerful set of inductive biases while greatly simplifying the query process. Our work differs from many previous works [3, 18, 33] that embed graphs into vector spaces, which leave the embedding space unstructured. In contrast, order embeddings have properties that naturally correspond to many properties of subgraph relationships, such as transitivity, symmetry and closure under intersection. Enforcing the order embedding constraint both leads to a well-structured embedding space and also allows us to efficiently navigate it in order to find subgraphs as well as supergraphs (Fig. 1).

NeuroMatch trains a Siamese graph neural network to learn the order embedding, and uses a max-margin loss to ensure that the subgraph relationships are captured. Importantly, NeuroMatch only needs to train the GNN once and can then use it on any target as well as query graphs. Furthermore, the embedding stage can be conducted *offline*, producing precomputed embeddings for the query stage. The query stage is extremely efficient as it only requires linear time both in the size of the query and the target graphs. And last, NeuroMatch generalizes naturally to graphs which include categorical node and edge features, as well as multiple target graphs.

We experiment with synthetic and real-world datasets and compare the accuracy and speed of NeuroMatch with state-of-the-art combinatorial methods for subgraph matching [8, 5] as well as recent neural methods for graph matching, which we adapted for the subgraph matching problem. Experiments show that NeuroMatch runs two orders of magnitude faster than combinatorial approaches and can scale to much larger query graphs. Compared to neural graph matching methods, NeuroMatch achieves an 18% improvement in AUROC for subgraph matching, and is able to identify locations of matches in much larger target graphs.

2. NeuroMatch Architecture

2.1. Problem Setup

We first describe the general problem of subgraph matching. Let $G_T = (V_T, E_T)$ be a large *target graph* where we aim to identify the query graph. Let X_T be the associated categorical node features

Algorithm 1: NeuroMatch Query Stage

Input: Target graph G_T , graph embeddings Z_u of node $u \in G_T$, and query graph G_Q .

Output: Subgraph of G_T that is isomorphic to G_Q .

- 1: For every node $q \in G_Q$, create G_q , and embed its center node q .
 - 2: Compute matching between embeddings Z_q and embeddings Z_T using subgraph prediction function $f(z_q, z_u)$.
 - 3: Use voting to decide the final matches.
-

for all nodes in V^1 . Let $G_Q = (V_Q, E_Q)$ be a *query graph* with associated node features X_Q . The goal of a subgraph matching algorithm is to identify the set of all subgraphs $\mathcal{H} = \{H | H \subseteq G_T\}$ that are isomorphic to G_Q , that is, \exists bijection $f : V_H \mapsto V_Q$ such that $(f(v), f(u)) \in E_Q$ iff $(v, u) \in E_H$. Furthermore, we say G_Q is a subgraph of G_T if \mathcal{H} is non-empty. When node and edge features are present, the subgraph isomorphism further requires that the bijection f has to match these features.

In the literature, subgraph matching commonly refers to two subproblems: node-induced matching and edge-induced matching. In node-induced matching, the set of possible subgraphs of G_T are restricted to graphs $H = (V_H, E_H)$ such that $V_H \subseteq V_T$ and $E_H = \{(u, v) | u, v \in V_H, (u, v) \in E_T\}$. Edge-induced matching, in contrast, restricts possible subgraphs by $E_H \subseteq E_T$, and contains all nodes that are incident to edges in E_H . To demonstrate, here we consider the more general edge-induced matching, although NeuroMatch can be applied to both.

In this paper, we investigate the following problems of subgraph matching.

Problem 1. Matching neighborhoods. Given a neighborhood G_u of u and query G_Q containing q , make binary prediction of whether G_Q is a subgraph of G_u where node q corresponds to u .

Problem 2. Matching query on datasets. Given a target graph G_T and a query G_Q , identify one or more appearances of G_Q in G_T .

In the first problem, we balance the number of positive and negative pairs of node neighborhoods in training and testing. The second problem requires prediction of subgraph relationship between the query and every node neighborhood in G_T .

2.2. Overview of NeuroMatch

NeuroMatch adopts a two stage process: *embedding stage* where G_T is decomposed into many small overlapping graphs and each graph is embedded. And the *query stage* where query graph is compared to the target graph directly in the embedding space so no expensive combinatorial search is required.

Embedding stage. In the embedding stage, NeuroMatch decomposes target graph G_T into many small overlapping graphs G_u and uses a Siamese graph neural network to embed them. For every node u in G_T , we extract the k -hop neighborhood of u , G_u (Figure 1). GNN then maps node u (that is, the structure of its network neighborhood G_u) into an embedding z_u .

Note a subtle but an important point: By using a k -layer GNN to embed node u , we are essentially embedding/capturing the k -hop network neighborhood structure G_u around the center node u . Thus, embedding u is equivalent to embedding G_u (a k -hop subgraph centered at node u), and by comparing embeddings of two nodes u and v , we are essentially comparing the structure of subgraphs G_u, G_v .

Query stage (Alg. 1). The goal of the query stage is to determine whether G_Q is a subgraph of G_T and identify the mapping of nodes of G_Q to nodes of G_T . However, rather than directly solving this problem, we develop a fast routine to determine whether G_q is a subgraph of G_u : We design a *subgraph prediction function* $f(z_q, z_u)$ that *predicts* whether the k -hop network neighborhood of node $u \in G_T$ is a subgraph of the k -hop neighborhood of node $q \in G_Q$. In other words, whether G_q is a subgraph of G_u . We thus formulate the subgraph matching problem as a node-level task by using $f(z_q, z_u)$ to predict the set of nodes v that can be matched to node q (that is, find a set of graphs G_u that are super-graphs of G_q). To determine whether G_Q is a subgraph of G_T , we then use a special voting mechanism where we select multiple center nodes $q \in G_Q$ (that is, create multiple G_q) and multiple center nodes $u \in G_T$ and combine predictions of $f(z_q, z_u)$ via voting.

Practical considerations and design choices. Experimentally we find that if we pick the center node to be the central node of the query graph, the performance tends to be significantly better. This

¹We consider the case of a single target and query graph, but NeuroMatch trivially applies to any number of target/query graphs.

is due to the smaller number of GNN message passing steps needed to capture the structure of the query graph. The choice of the number of layers, k , depends on the size of the query graphs. We assume k is at least the diameter of the query graph, to allow the information of all nodes to be propagated to the center node in the query. In experiments, however, we observe that inference via voting can still produce reliable matchings even with k less than the query graph diameter.

NeuroMatch is flexible in terms of the GNN model used for the embedding step. We adopt a variant of GIN [32] incorporating skip layers to encode the query graphs and the neighborhoods, which has strong theoretical guarantees and shows empirical performance advantages.

2.3. Subgraph Prediction Function $f(z_q, z_u)$

Given the target graph node embeddings z_u and the center node $q \in G_Q$, the subgraph prediction function decides if $u \in G_T$ has a k -hop neighborhood that is subgraph isomorphic to q 's k -hop neighborhood in G_Q . The key is that subgraph prediction function makes this decision based only on the embeddings z_q and z_u of nodes q and u (Figure 1).

Capturing subgraph relations in the embedding space. We enforce the embedding geometry to directly capture subgraph relations. This approach has the additional benefit of ensuring that the subgraph predictions have negligible cost at the query stage, since we can just compare the coordinates of two node embeddings. In particular, NeuroMatch satisfies the following properties for subgraph relations (Refer to Appendix for proofs of the properties):

- *Transitivity:* If G_1 is a subgraph of G_2 and G_2 is a subgraph of G_3 , then G_1 is a subgraph of G_3 .
- *Anti-symmetry:* If G_1 is subgraph of G_2 , G_2 is a subgraph of G_1 iff they are isomorphic.
- *Intersection set:* The intersection of the set of G_1 's subgraphs and the set of G_2 's subgraphs contains all common subgraphs of G_1 and G_2 .
- *Non-trivial intersection:* The intersection of any two graphs contains at least the trivial graph.

We use the notion of set embeddings [19] to capture these inductive biases. Common examples include order embeddings and box embeddings. In contrast to Euclidean point embeddings, set embeddings enjoy many properties that correspond naturally to the subgraph relations.

Subgraph prediction function. The idea of order embeddings is illustrated in Figure 1. Order embeddings ensure that the subgraph relations are properly reflected in the embedding space: if G_q is a subgraph of G_u , then the embedding z_q of node q has to be to the ‘‘lower-left’’ of u 's embedding z_u :

$$z_q[i] \leq z_u[i] \forall_{i=1}^D \quad \text{iff} \quad G_q \subseteq G_u \quad (1)$$

where D is the embedding dimension. We thus train the GNN that produces the embeddings using the max margin loss:

$$\mathcal{L}(z_q, z_u) = \sum_{(z_q, z_u) \in P} E(z_q, z_u) + \sum_{(z_q, z_u) \in N} \max\{0, \alpha - E(z_q, z_u)\}, \text{ where} \quad (2)$$

$$E(z_q, z_u) = \|\max\{0, z_q - z_u\}\|_2^2 \quad (3)$$

Here P denotes the set of positive examples in minibatch where the neighborhood of q is a subgraph of neighborhood of u , and N denotes the set of negative examples. A violation of the subgraph constraint happens when in any dimension i , $z_q[i] > z_u[i]$, and $E(z_q, z_u)$ represents its magnitude. For positive examples P , $E(z_q, z_u)$ is minimized when all the elements in the query node embedding z_q are less than the corresponding elements in target node embedding z_u . For negative pairs (z_q, z_u) the amount of violation $E(z_q, z_u)$ should be at least α , in order to have zero loss.

We further use a threshold t on the violation $E(z_q, z_u)$ to make decision of whether the query is a subgraph of the target. The subgraph prediction function f is defined as:

$$f(z_q, z_u) = \begin{cases} 1 & \text{iff } E(z_q, z_u) < t \\ 0 & \text{otherwise} \end{cases} \quad (4)$$

Subgraph constraint supervision at every layer. To satisfy the composition property, we enforce that subgraph constraints at all layers. We show in the Appendix that this corresponds to satisfying the composition property. Subgraph constraints from the first layer to the last layer are enforced by adding a max-margin loss component corresponding to each layer.

For layer k and for all matching pairs of nodes $q \in G_Q$ and $u \in G_T$, we compute the loss in Equation 2 by taking the current layer embedding of q and u : $\mathcal{L}_k = \mathcal{L}(h_q^k, h_u^k)$. The final loss is then $\mathcal{L}_{\text{final}} = \sum_{k=1}^K \mathcal{L}_k + \lambda \mathcal{L}(z_q, z_u)$, where λ controls the importance of intermediate subgraph constraints with respect to the last layer subgraph constraint.

2.4. Matching Nodes via Voting

At the query time, our goal is to predict if query node $q \in G_Q$ and target node $u \in G_T$ have subgraph-isomorphic k -hop neighborhoods G_q and G_u . That is, whether nodes q and u match.

Direct matching. The direct approach is to match nodes based on their embeddings. Specifically, we use the subgraph prediction function $f(z_q, z_u)$ to predict the subgraph relation between q and u .

Matching via voting (Alg. 2). To improve on the direct match we propose a voting method that improves the accuracy of matching a pair of nodes based on their neighboring nodes. Our insight is that matching a pair of nodes imposes constraints on the neighborhood structure of the pair. Therefore, we can use the embeddings of the neighboring nodes of the node pair to augment the prediction.

Suppose we want to predict if node $q \in G_Q$ and node $u \in G_T$ match. We have:

Observation 1. Let $\mathcal{N}^{(k)}(u)$ denote the k -hop network neighborhood of node u . Then, if $q \in G_Q$ and node $u \in G_T$ match, then for all nodes $i \in \mathcal{N}^{(k)}(q)$, \exists node $j \in \mathcal{N}^{(l)}(u)$, $l \leq k$ such that node i and node j match.

Refer to the proof in Appendix. Based on this observation, we propose a voting-based inference method. Suppose that node $u \in G_Q$ matches node $v \in G_T$. We check if all neighbors of node u satisfy Observation 1, i.e. each neighbor of u has a match, as is summarized in Algorithm 2.

2.5. Training NeuroMatch

The training of subgraph matching consists of the following component: (1) Sample training query G_Q from target graph G_T . (2) Sample node q and neighborhood G_q in G_Q and find q 's corresponding node u and its $G_u \subseteq G_T$. (3) Generate negative example w and its $G_w \subseteq G_T$. (4) Compute node embeddings for q, u, w with GNN, and the loss in Equation 2 for backprop. We now detail the following components in this training process.

Training data generation. In order to achieve good generalization performance on unseen target and query graphs, we train the network on randomly generated query graphs. We generate training examples by sampling random subgraphs of the large target graph G_T , as follows. We randomly select a node $u \in G_T$ to use as our center node. Starting from u , we do a breadth-first traversal of the graph, randomly traversing each edge in BFS with some probability. The search terminates at k hops away from the center node, after which the traversed edges from the target graph form the query graph G_Q . Such process generates a pair of positive examples: the sampled subgraph G_Q , and the k -hop neighborhood of the center node u .

Curriculum learning. We introduce a curriculum training scheme that improves model performance. We first train the model on a small number of easy queries and then train on successively more complex queries with increased batch size. The curriculum is initialized with a single 1 hop query. Each time the training performance plateaus below a threshold loss, the size of the query is increased by one, up to a maximum of K hops. After reaching a K hop query, the number of queries that the model is trained on is doubled each time the loss plateaus again, up to a maximum of 256 queries. We find empirically that 256 queries is sufficient for the model to learn the general matching task rather than overfitting to the

Algorithm 2: NeuroMatch Voting Algorithm

Input: Query node $q \in G_Q$, target node $u \in G_T$.

Threshold t for violation below which we predict positive subgraph relation between the neighborhoods of q and u .

Output: Whether the node pair matches.

Compute embeddings for neighbors of q, u within K hops

for hop $k \leq K$ **do**

for node $i \in \mathcal{N}^{(k)}(q)$ **do**

$m = \min\{E(z_i, z_j) | \forall j \in \mathcal{N}^{(k)}(u)\}$

If $m > t$, **return** False

return True

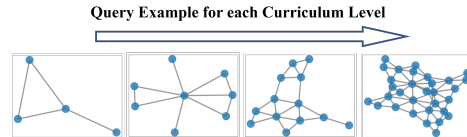


Figure 2: Example queries G_Q at each level of the curriculum in the MSRC_21 dataset. The diameter and number of nodes increase as curriculum level advances.

	Dataset	E-R	COX2	DD	MSRC_21	FIRSTMMDB	PPI	WORDNET18
Base	GMNN [33]	73.6 ± 1.1	75.9 ± 0.8	80.6 ± 1.5	82.5 ± 1.7	81.5 ± 2.9	72.0 ± 1.9	80.3 ± 2.0
	RDGCN [31]	79.5 ± 1.2	80.1 ± 0.4	81.3 ± 1.2	81.9 ± 1.9	82.4 ± 3.4	76.8 ± 2.2	79.6 ± 2.5
Ablation	NO CURRICULUM	82.4 ± 0.6	95.0 ± 1.6	96.7 ± 2.1	89.2 ± 2.0	87.2 ± 6.8	82.6 ± 1.7	81.4 ± 2.2
	NM-MLP	88.7 ± 0.5	95.4 ± 1.6	98.4 ± 0.3	93.5 ± 1.0	92.9 ± 4.3	85.5 ± 1.4	87.9 ± 1.2
	NM-NTN	89.1 ± 1.9	89.3 ± 0.9	96.4 ± 1.4	94.7 ± 3.2	89.6 ± 1.1	85.7 ± 2.4	85.0 ± 1.1
	NM-BOX	84.5 ± 2.1	88.5 ± 1.2	91.4 ± 0.5	90.8 ± 1.4	93.8 ± 1.8	77.4 ± 3.1	82.7 ± 2.5
	NEUROMATCH	93.5 ± 1.1	97.2 ± 0.4	97.5 ± 1.2	96.1 ± 0.2	95.5 ± 2.1	89.9 ± 1.9	89.3 ± 2.4

Table 1: Given a neighborhood G_u of u and query G_Q containing q , make binary prediction of whether G_u is a subgraph of G_u where node q corresponds to u . We report AUROC (unit 0.01). NeuroMatch performs the best with median AUROC 95.5, 20% higher than the neural baselines.

specific queries in the training set. Figure 2 shows examples of queries at each curriculum level. The complexity of the query increases as training proceeds.

Negative Sampling. We also employ negative sampling to speed-up training. Given a positive pair of query and target graph, we generate three types of negative examples. The first type of negative examples are created by pairing a query with a target graph corresponding to a different query. The second type of negatives are created by randomly choosing a different node in the same target graph and using its k -hop neighborhood as a target graph. The second type is harder, because it requires the model to distinguish potentially overlapping neighborhoods at a node level. The second case also improves model’s performance when matching all nodes in a query to nodes in the target graph. The third type of negatives are generated by perturbing the query to make it no longer a subgraph of the target graph. This creates a negative example which is topologically similar to the target graph. These are the hardest negative examples used to encourage the model to better learn to predict subgraph relation via graph topology.

2.6. Discussion and Design Alternatives

There are many benefits of NeuroMatch, when applied to subgraph matching tasks, both in terms of performance and runtime complexity.

Runtime complexity. The embedding stage uses GNNs to train embeddings to obey the subgraph constraint. Its complexity is $O(K(|E_T| + |E_Q|))$, where K is the number of GNN layers. In the query stage, if we want to identify all matches between the query and the target graph, we need to compute a total of $O(|V_T||V_Q|)$ scores.

In many use cases, the target graphs are available in advance, but we need to solve for new incoming unseen queries. Prior to inference time, the embeddings for all nodes in the target graph can be pre-computed with complexity $O(K|E_T|)$. For a new query, its node embeddings can be computed in $O(K|E_Q|)$ time, which is much faster since queries are smaller. With order embedding, we do not need additional neural network modules at query stage and simply compute the order relations between query node embeddings and the pre-computed node embeddings in the target graph.

Alternative geometric embeddings. An alternative design choice for geometric embeddings are box embeddings [28]. Compared to order embeddings, box embeddings have an additional degree of freedom, and can be specified by two vectors: the box center and the box size. Box embeddings model subgraph relation by containment: Graph A is a subgraph of graph B if the embedding box of A is entirely contained in the embedding box of B . Although it has higher flexibility, box embeddings no longer satisfy the intersection set property, since two boxes can be completely disjoint.

3. Experiments

To investigate the effectiveness of NeuroMatch, we compare its runtime and performance with a range of existing popular subgraph matching methods. We evaluate performance on synthetic datasets to probe data efficiency and generalization ability, as well as a variety of real-world datasets spanning many fields to evaluate whether the model can be adapted to real-world graph structures.

3.1. Datasets and Baselines

Synthetic dataset. We use Erdős-Rényi (ER) random graphs [10]. At training time, we generate target graphs and queries as random ER graphs. At test time, we evaluate on test query graphs that were not seen during training. See Appendix for dataset details, where we also show experiments to transfer the learned model to unseen real dataset without fine-tuning.

Real-world datasets. We use a variety of real-world datasets from different domains. We evaluate on graph benchmarks in chemistry (COX2), biology (DD, PPI networks), image processing (MSRC_21), point cloud (FIRSTMMDB), and knowledge graph (WORDNET18). We do not include node features for PPI networks since the goal is to match various protein interaction patterns without considering the identity of proteins. WORDNET18 contains no node features, but we use its edge types information in matching. For all other datasets, we require that the matching takes categorical features of nodes into account. Refer to the Appendix for statistics of all datasets. For all datasets, query graphs are generated by random sampling of subgraphs with size 20-50 in the datasets. First row of the result tables indicates the datasets used for each experiment.

Baselines. We first consider popular existing combinatorial approaches. We adopt the most commonly used efficient methods: the VF2 [8] and the RI algorithm [5].

There are currently no neural methods specifically used for subgraph matching. We therefore adapt two existing state-of-the-art methods for graph matching, Graph Matching Neural Networks (GMNN) [33] and RDGCN [31], by changing their objective from predicting whether two graphs have a match to predicting the subgraph relation. Compared to NeuroMatch, both methods are computationally more expensive due to cross-graph attention between nodes.

Training details. We train the algorithm for 10K epochs, and use the epoch with the best validation result for testing. See Appendix for hardware usage and hyperparameter configurations.

3.2. Results

(1) Matching individual node network neighborhoods. Table 1 summarizes the AUROC results for predicting subgraph relation for Problem 1: is node q 's k -hop neighborhood G_q a subgraph of u 's neighborhood G_u . The number of pairs G_q, G_u with positive labels is equal to the number of pairs with negative labels. We observe that NeuroMatch with order embeddings obtains, on average, a 20% improvement over neural baselines. This benefit is a result of avoiding the loss of information when pooling node embeddings and a better inductive bias stemming from order embeddings.

(2) Ablation studies. Although learning subgraph matching has not been extensively studied, we explore alternatives to components of NeuroMatch. We compare with the following variants:

- NO CURRICULUM: Same as NEUROMATCH but with no curriculum training scheme.
- NM-MLP: uses MLP and cross entropy to replace the order embedding loss.
- NM-NTN: uses Neural Tensor Network [23] and cross entropy to replace order embedding loss.
- NM-BOX: uses box embedding loss [28] to replace the order embedding loss.

As shown in Table 1, box embeddings cannot guarantee intersection, *i.e.* common subgraphs, between two graphs. The variable sizes of the target graph makes dimension interactions hard to learn, hence the NTM variant does not perform the best.

We additionally observe that the learning curriculum is crucial to the performance of learning the subgraph relationships. The use of the curriculum increases the performance by an average of 6%, while significantly reducing the performance variance and increasing the convergence speed. This benefit is due to the compositional nature of the subgraph matching task.

(3) Identifying all pairs of matching nodes. In Table 2, instead of predicting the subgraph relation between q 's neighborhood and u 's neighborhood, we predict the entire isomorphism mapping between the G_Q and G_u : If node $q' \in G_Q$ matches $u' \in G_u$, $f(z_{q'}, z_{u'})$ should predict 1. Graph matching baselines such as GMNN and RDGCN are not applicable, since they use aggregated graph embeddings, and do not consider the case where a node can be mapped to multiple nodes.

NeuroMatch performs subgraph matching at the node level, and hence is able to predict the isomorphism mapping. This is a harder task compared to matching only q and u 's neighborhoods, because more message passing steps are required to propagate information to all nodes (equal to the diam-

Dataset	E-R	COX2	DD	MSRC_21	FIRSTMMDB
NEUROMATCH	94.2 ± 0.4	88.5 ± 2.4	84.5 ± 2.9	83.3 ± 2.1	92.8 ± 4.1

Table 2: Given u 's neighborhood G_u and its subgraph G_Q , make binary prediction for every $q \in G_Q$ and its corresponding node $v \in G_u$. The AUROC (unit: 0.01). GMNN and RDGCN do not apply here since they cannot match query nodes to a subset of nodes in the target (See Appendix for ablation studies).

Dataset	COX2	DD	MSRC_21	FIRSTMMDB
NM-MLP	48.5 ± 1.1	52.6 ± 0.8	42.3 ± 1.1	35.1 ± 0.6
NEUROMATCH	55.2 ± 1.4	59.8 ± 1.0	51.5 ± 0.8	48.5 ± 0.9

Table 3: Hit at 3 when matching test queries to the entire dataset. Given G_Q as a subgraph of G_T , where $q \in G_Q$ corresponds to $u \in G_T$, evaluate the percentage of times where u is ranked as top-3 most likely node whose neighborhood contains G_Q as a subgraph.

eter of the neighborhoods). Table 2 shows that correspondence between all nodes in query G_Q and all nodes in G_T can be computed reliably, although the performance is 3% lower compared to Table 1.

(4) Matching query to the entire target graph . Given a target G_T , we randomly sample a query G_Q centered at q . The goal is to find G_Q in G_T . For all nodes in G_T , we rank them by their violation scores $E(z_q, z_u)$. The lower the score, the more certain is the model that G_Q is a subgraph of the neighborhood of u . We pick the top 3 nodes in G_T with the lowest scores, and evaluate the percentage of times when the groundtruth u is contained in the predicted top 3 nodes, *i.e.* the hit at 3 metric. Note that measuring recall requires exact subgraph matching which is very expensive for our queries of sizes between 20 to 50. Unlike the previous tasks, it requires prediction of subgraph relations between G_Q and neighborhoods G_u for all $u \in G_T$.

Table 3 shows the Hits@3 performance of NeuroMatch. The baseline graph matching algorithm do not apply, since they do not find the location(s) of the query subgraph. Matching queries to very large target graphs is still a challenging task due to the overwhelming prevalence of negative examples. Hence hit at K becomes a challenging metric since it’s very hard for the model to rank the correct match higher than very large number of negative examples (nodes that do not correspond to q) in the target graph.

We further investigate the confusion matrix (see Appendix) for the DD dataset for small test queries (constrained to ≤ 10 nodes where computing recall by exact matching is tractable), which shows extreme imbalance (positive subgraph relations consist of 6% of the label). However, our model is still able to eliminate 88.3% of the false target graphs. Running heuristic matching to confirm the filtered positive would mean at least a 10x speedup compared to running heuristics on all graphs.

Inference speed comparison. We further perform runtime comparison. We run VF2 and RI on the same test queries of the DD and MSRC_21 datasets, along with synthetic Erdős-Rényi graphs. If the subgraph matching heuristics runs for more than 40 seconds, it is deemed as unsuccessful. We show in Appendix the Figure of the success rate of the baselines, which drop below 60% when the query size is increased to more than 50. We additionally record the average runtime of each baseline algorithm and compare with NeuroMatch. We provide both our baselines and NeuroMatch with the same 10000 test queries and measure their average runtime. In terms of runtime, our order embedding variant is 10 times more efficient compared to the MLP variant (See Table 4), and more than 100 times more efficient than exact algorithms.

4. Related Work

Structural and semantic (sub)graph matching. In its most general form, a match of a query to a subgraph of the target graph requires comparison of their structure and semantic features [12]. Conventional algorithms such as [26] focus on graph structures only. Other works [1, 7] also consider categorical node features and perform subgraph matching with the constraint that matched pairs of node need to have the same label. Our NeuroMatch can operate under both settings.

Optimal and approximate algorithms. Aside from search algorithms that return the exact matching for a subgraph matching instance, approximate solutions have also been proposed [6, 27] that run in polynomial time, but are not guaranteed to find the correct solution. Our NeuroMatch is related in a sense that it is approximate algorithm but improves existing algorithms in scalability, performance, and the ability to apply to many variants of the subgraph isomorphism problem.

Neural graph matching. Recently, Siamese graph neural networks [16, 15, 32] have been proposed for graph isomorphism [3, 18, 14] and have achieved state-of-the-art results [35, 29, 33]. However, these methods cannot be directly employed in subgraph isomorphism since there is no one-to-one correspondence between nodes in query and search graphs. We demonstrate that our contributions in using node-based representations, geometric set embedding space and voting of matched nodes can significantly outperform direct applications of graph matching methods in the subgraph isomorphism setting. Additionally, recent works [4, 11] provide solutions to compute discrete matching from the neural prediction of isomorphism mapping and are complementary to our work.

Datasets	E-R	MSRC_21	DD
VF2	25.9	19.7	22.8
RI	12.8	7.5	11.0
NEUROMATCH-MLP	0.49	0.48	0.44
NEUROMATCH-ORDER	0.04	0.03	0.03

Table 4: Average runtime (in seconds) comparison between heuristic methods and our method with query size up to 50. NeuroMatch is about 100x faster than alternatives.

5. Conclusion

In this paper we presented a neural subgraph matching algorithm, NeuroMatch, that uses graph neural networks and geometric embeddings to achieve state-of-the-art performance in learning to match query graphs to large target graphs. We observe that order embeddings are a natural fit to model subgraph relationships in the embedding space of graphs. NeuroMatch is the first subgraph matching algorithm that out-performs adaptations of existing graph-isomorphism related architectures. Compared to existing heuristics algorithms, NeuroMatch exhibits a 100x speedup at query time.

6. Broader Impact

Subgraph matching is a problem of fundamental theoretical importance in computer science, and finds applications in a broad range of disciplines where graph processing arises. In social science, social networks are commonly modeled as large graphs, and subgraph analysis has played an important role in the analysis of network effects [17]. Information retrieval systems use subgraph structures in knowledge graphs for semantic summarization, analogy reasoning, and relationship prediction [13, 24]. In chemistry, subgraph matching is a robust and accurate method for determining similarity between chemical compounds, a necessary precursor for recent methods in chemical retrosynthesis as well as analysis of complex chemical reactions in systems biology [21, 9]. Elsewhere in biology, subgraph matching is of central importance in the analysis of protein-protein interaction networks, where identifying and predicting functional motifs is a primary tool for understanding biological mechanisms such as those underlying disease, aging, and medicine [2, 22]. An efficient, accurate model for the subgraph matching problem such as NeuroMatch could drive research in all of these domains, by providing insights into important substructures of these networks, which have traditionally been limited by either the quality of their approximate algorithms or the runtime of exact algorithms.

While the model itself is widely applicable, its application into these disciplines requires caution. Since queries are typically determined at inference time, it is easy for human biases (based on observed inference data) to leak into the queries and bias results, confirming hypotheses while missing other important subgraph patterns which do not support the hypothesis. Moreover, a GNN-generated output should be treated with the same scrutiny as any other research result; our model is still imperfect and likely always will be. With the deleterious societal effects of automation bias and algorithmic bias becoming increasingly clear, care must be taken to ensure that results are validated with due diligence.

From a theoretical perspective, our work additionally demonstrates the possibility to learn accurate models for NP-hard problems on graphs. Hence, it could inspire other high-performance GNN-based approaches to similar hard graph problems such as vertex cover, independent set, Hamiltonian paths, *etc.*. These problems are widely used in areas such as operations research, computer systems and architecture. Future work in these related problems has the potential to revolutionize these fields.

7. Acknowledgement

The authors acknowledge Andrew Wang (awang@stanford.edu) for helping with code organization and integration with the PyTorch Geometric and DeepSNAP libraries. We gratefully acknowledge the support of DARPA under Nos. FA865018C7880 (ASED), N660011924033 (MCS); ARO under Nos. W911NF-16-1-0342 (MURI), W911NF-16-1-0171 (DURIP); NSF under Nos. OAC-1835598 (CINES), OAC-1934578 (HDR), CCF-1918940 (Expeditions), IIS-2030477 (RAPID); Stanford Data Science Initiative, Wu Tsai Neurosciences Institute, Chan Zuckerberg Biohub, Amazon, Boeing, Chase, Docomo, Hitachi, Huawei, JD.com, NVIDIA, Dell. J. L. is a Chan Zuckerberg Biohub investigator. The U.S. Government is authorized to reproduce and distribute reprints for Governmental purposes notwithstanding any copyright notation thereon. Any opinions, findings, and conclusions or recommendations expressed in this material are those of the authors and do not necessarily reflect the views, policies, or endorsements, either expressed or implied, of DARPA, NIH, ARO, or the U.S. Government.

References

- [1] B. Aleman-Meza, C. Halaschek-Wiener, S. S. Sahoo, A. Sheth, and I. B. Arpinar. Template based semantic similarity for security applications. In *International Conference on Intelligence and Security Informatics*. Springer, 2005.
- [2] N. Alon, P. Dao, I. Hajirasouliha, F. Hormozdiari, and S. C. Sahinalp. Biomolecular network motif counting and discovery by color coding. *Bioinformatics*, 2008.
- [3] Y. Bai, H. Ding, S. Bian, T. Chen, Y. Sun, and W. Wang. Simgnn: A neural network approach to fast graph similarity computation. In *WSDM*. ACM, 2019.
- [4] Y. Bai, H. Ding, Y. Sun, and W. Wang. Convolutional set matching for graph similarity. In *NeurIPS*, 2018.
- [5] V. Bonnici, R. Giugno, A. Pulvirenti, D. Shasha, and A. Ferro. A subgraph isomorphism algorithm and its application to biochemical data. *BMC bioinformatics*, 2013.

- [6] W. J. Christmas, J. Kittler, and M. Petrou. Structural matching in computer vision using probabilistic relaxation. *PAMI*, 1995.
- [7] T. Coffman, S. Greenblatt, and S. Marcus. Graph-based technologies for intelligence analysis. *Communications of the ACM*, 2004.
- [8] L. P. Cordella, P. Foggia, C. Sansone, and M. Vento. A (sub) graph isomorphism algorithm for matching large graphs. *PAMI*, 2004.
- [9] H. Dai, C. Li, C. Coley, B. Dai, and L. Song. Retrosynthesis prediction with conditional graph logic network. In *NeurIPS*, 2019.
- [10] P. Erdős and A. Rényi. On the evolution of random graphs. *Publ. Math. Inst. Hung. Acad. Sci.*, 1960.
- [11] M. Fey, J. E. Lenssen, C. Morris, J. Masci, and N. M. Kriege. Deep graph matching consensus. In *ICLR*, 2020.
- [12] B. Gallagher. Matching structure and semantics: A survey on graph-based pattern matching. In *AAAI Fall Symposium*, 2006.
- [13] D. Gentner. Structure-mapping: A theoretical framework for analogy. *Cognitive science*, 1983.
- [14] M. Guo, E. Chou, D.-A. Huang, S. Song, S. Yeung, and L. Fei-Fei. Neural graph matching networks for fewshot 3d action recognition. In *ECCV*, 2018.
- [15] W. Hamilton, Z. Ying, and J. Leskovec. Inductive representation learning on large graphs. In *NeurIPS*, 2017.
- [16] T. N. Kipf and M. Welling. Semi-supervised classification with graph convolutional networks. In *ICLR*, 2017.
- [17] J. Leskovec, A. Singh, and J. Kleinberg. Patterns of influence in a recommendation network. In *PAKDD*. Springer, 2006.
- [18] Y. Li, C. Gu, T. Dullien, O. Vinyals, and P. Kohli. Graph matching networks for learning the similarity of graph structured objects. In *ICML*, 2019.
- [19] B. McFee and G. Lanckriet. Partial order embedding with multiple kernels. In *ICML*. ACM, 2009.
- [20] E. Plotnick. *Concept mapping: A graphical system for understanding the relationship between concepts*. ERIC Clearinghouse on Information and Technology Syracuse, NY, 1997.
- [21] J. W. Raymond, E. J. Gardiner, and P. Willett. Heuristics for similarity searching of chemical graphs using a maximum common edge subgraph algorithm. *Journal of chemical information and computer sciences*, 2002.
- [22] R. Shen, N. C. Goonesekere, and C. Guda. Mining functional subgraphs from cancer protein-protein interaction networks. *BMC systems biology*, 2012.
- [23] R. Socher, D. Chen, C. D. Manning, and A. Ng. Reasoning with neural tensor networks for knowledge base completion. In *NeurIPS*, 2013.
- [24] Q. Song, Y. Wu, P. Lin, L. X. Dong, and H. Sun. Mining summaries for knowledge graph search. *IEEE Transactions on Knowledge and Data Engineering*, 2018.
- [25] Z. Sun, H. Wang, H. Wang, B. Shao, and J. Li. Efficient subgraph matching on billion node graphs. *Proceedings of the VLDB Endowment*, 2012.
- [26] J. R. Ullmann. An algorithm for subgraph isomorphism. *Journal of the ACM (JACM)*, 1976.
- [27] S. Umeyama. An eigendecomposition approach to weighted graph matching problems. *PAMI*, 1988.
- [28] L. Vilnis, X. Li, S. Murty, and A. McCallum. Probabilistic embedding of knowledge graphs with box lattice measures. *ACL*, 2018.
- [29] R. Wang, J. Yan, and X. Yang. Learning combinatorial embedding networks for deep graph matching. In *ICCV*, 2019.
- [30] J. Winn, A. Criminisi, and T. Minka. Object categorization by learned universal visual dictionary. In *ICCV*. IEEE, 2005.
- [31] Y. Wu, X. Liu, Y. Feng, Z. Wang, R. Yan, and D. Zhao. Relation-aware entity alignment for heterogeneous knowledge graphs. 2019.

- [32] K. Xu, W. Hu, J. Leskovec, and S. Jegelka. How powerful are graph neural networks? *ICLR*, 2018.
- [33] K. Xu, L. Wang, M. Yu, Y. Feng, Y. Song, Z. Wang, and D. Yu. Cross-lingual knowledge graph alignment via graph matching neural network. 2019.
- [34] Q. Yang and S.-H. Sze. Path matching and graph matching in biological networks. *Journal of Computational Biology*, 2007.
- [35] Z. Zhang and W. S. Lee. Deep graphical feature learning for the feature matching problem. In *ICCV*, 2019.

Code associated with this submission can be found at: https://drive.google.com/file/d/1YPEdo4tkm0lZr-4OUR28yb1Fps_t2Cbz/view?usp=sharing.

A. Order Embedding Space

Figure 3 shows the TSNE embedding of the order embedding space (64 dimensions) when trained on the synthetic dataset. The yellow color points correspond to embeddings of graphs with larger sizes; the purple color points correspond to embeddings of graphs with smaller sizes. Red points are example embeddings for which we also visualize the corresponding graphs (center node not visualized). We observe that the order constraints are well-preserved. Accordingly, if there is no subgraph relations between two graphs, their embeddings violate the order constraint.

Furthermore, the common subgraph relation is also easily obtained from the embedding space. For example, Graph *C* is a common subgraph of graph *E* and *F*. Hence in the embedding space, *C* is below and to the left of the elementwise minimum of *E* and *F*.

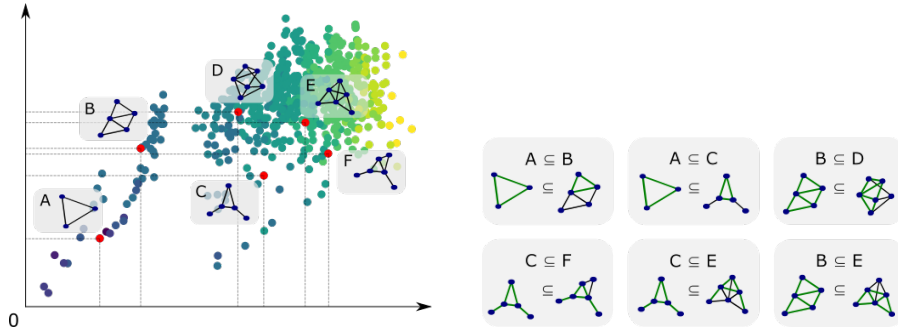


Figure 3: Example order embedding for a subset of subgraphs sampled from the ENZYMES dataset. Graphs that are below and to the left of a given graph are subgraphs of that graph. For example, graphs *A*, *B* and *C* are all subgraphs of *E*. Graphs are colored by size (number of edges they contain).

B. Proof of Subgraph Properties

The subgraph properties in Section 3.3 are direct consequences of the subgraph definition. All the properties are also satisfied with our center node definition. We show the proofs for the properties with the center node correspondence.

Transitivity. Suppose that G_1 is a subgraph of G_2 with bijection f mapping all nodes from G_1 to a subset of nodes in G_2 , and G_2 is a subgraph of G_3 with bijection g . Let v_1, v_2, v_3 be the corresponding nodes in G_1, G_2, G_3 respectively. Then the composition $g \circ f$ is a bijection. Moreover, $g \circ f(v_1) = g(v_2) = v_3$. Therefore G_1 is a subgraph of G_3 , and thus the transitivity property.

This corresponds to the transitivity of order embedding.

Anti-symmetry. Suppose that G_1 is a subgraph of G_2 with bijection f , and G_2 is a subgraph of G_1 with bijection g . Then for any node $v \in G_1$, $g \circ f(v) = v$. g is the inverse mapping of f . By definition of isomorphism, G_1 and G_2 are isomorphic.

This corresponds to the anti-symmetry of order embedding.

Intersection. By definition, if G_3 is a common subgraph of G_1, G_2 , the G_3 is a subgraph of both G_1 and G_2 . Since a trivial edge is a subgraph of any graph, there is always a non-empty intersection set between two graphs.

Correspondingly, if $z_3 \preceq z_1$ and $z_3 \preceq z_2$, then $z_3 \preceq \min\{z_1, z_2\}$. Here \min denotes the element-wise minimum of two embeddings. Note that the order embedding z_1 and z_2 are positive, and therefore $\min\{z_1, z_2\}$ is another valid order embedding, corresponding to the non-empty intersection set between two graphs.

Finally, note that all properties hold when considering the center node correspondences between graphs.

C. Data Set Statistics

Biology and chemistry datasets. COX2 contains 467 graphs of chemical molecules with an average of 41 nodes and 44 edges each. DD contains 1178 graphs with an average of 284 nodes and 716 edges. It describes protein structure graphs where nodes are amino acids and edges represent positional proximity. We use node labels for both of the datasets. PPI dataset contains the protein-protein interaction graphs for human tissues. It has 24 graphs corresponding to different PPI networks of different human tissues. In total, there are 56944 nodes and 818716 edges. We do not include node features for PPI networks since the goal is to match various protein interaction patterns without considering the identity of proteins.

MSRC_21 is a semantic image processing dataset introduced in [30], containing 563 graph each representing the graphical model of an image. It has an average of 78 nodes and 199 edges.

FIRSTMMDB is a point cloud dataset containing 3d point clouds for various household objects. It contains 41 graphs with an average of 1377 nodes and 3074 edges each.

For all datasets, we randomly sample connected subgraph queries as test sets, with diameter less than 8, a mild assumption since most of the graph datasets have diameter less than 8.

D. Order embeddings

We can show that the order constraints in Equation 1 hold under the composition of multiple message passing layers of the GNN.

Suppose that we use a k -layer GNN to encode nodes u and v in the search and query graphs respectively. If the k -hop neighborhood of u is a subgraph of the k -hop neighborhood of v , then $\forall s \in \mathcal{N}_v, \exists t \in \mathcal{N}_u$ such that the $(k-1)$ -hop neighborhood of s must be a subgraph of the $(k-1)$ -hop neighborhood of t . Neighborhoods of u 's neighbors are subgraphs of a subset of the $(k-1)$ -hop neighborhoods of v 's neighbors.

Consequently, we can guarantee the following observation with order embeddings:

Observation 2. *Suppose that all GNN embeddings at layer $k-1$ satisfy order constraints after transformation. Then when using sum-based neighborhood aggregation, the GNN embeddings at layer k also satisfy the order constraints.*

After applying linear transformations and non-linearities in the GNN at layer $k-1$, if the order embedding of all neighbors of node v are no greater than that of the corresponding matched nodes in the target graph (*i.e.* satisfy the order constraint), then when summing the order embeddings of neighbors to compute embedding of v at layer k , it is guaranteed that node v also satisfies the order constraint at layer k . This corresponds to the property of composition of subgraphs into larger subgraphs.

E. Voting Procedure

The voting procedure is used to improve certainty of matched pairs by considering presence of nearby matched pairs in neighborhoods of the matched pairs. The method is motivated by the following observation.

Observation 3. *Let $\mathcal{N}^{(l)}$ denotes the l -hop neighborhood. Then, if $q \in G_Q$ and node $u \in G_T$ match, then for all nodes $i \in \mathcal{N}^{(k)}(q), \exists$ node $j \in \mathcal{N}^{(l)}(u), l \leq k$ such that node i and node j match.*

Since the query graph G_Q is a subgraph of target graph G_T , all paths in G_Q have corresponding paths in G_T . Hence the shortest distance of a node $i \in \mathcal{N}^{(k)}(q)$ to q is at most the shortest distance of node $j \in \mathcal{N}^{(l)}(u)$ in G_T , where j is the corresponding node in G_T defined by the subgraph isomorphism mapping. However, the shortest paths are not necessarily of equal lengths, since in G_T there might be additional short-cuts from j to u that do not exist in G_Q .

Model	Accuracy
SAGE (2-LAYER, 32-DIM, DROPOUT=0.2)	77.5
SAGE (6-LAYER, 32-DIM, DROPOUT=0.2)	85.3
SAGE (8-LAYER, 64-DIM, DROPOUT=0.2)	86.3
GCN (6-LAYER, 64-DIM, DROPOUT=0.2)	69.9
GCN (9-LAYER, 128-DIM, DROPOUT=0.2)	82.3
GIN (4-LAYER, 32-DIM, DROPOUT=0.2)	81.0
GIN (4-LAYER, 64-DIM, DROPOUT=0)	87.0
GIN (8-LAYER, 64-DIM, DROPOUT=0)	88.4
SAGE (4-LAYER, 64-DIM, DROPOUT=0)	87.6
SAGE (8-LAYER, 64-DIM, DROPOUT=0)	89.4
SAGE (12-LAYER, 64-DIM, DROPOUT=0)	90.5
SAGE (8-LAYER, 64-DIM, DROPOUT=0, SKIP-LAYER)	91.5

Table 5: The accuracy (unit: 0.01) for matching on the ENZYMES dataset for different model configurations.

F. Training details and hyperparameters

All models are trained on a single GeForce RTX 2080 GPU, and both the heuristics and neural models use a Intel Xeon E7-8890 v3 CPU.

Curriculum training. In each epoch, we iterate over all target graphs in the curriculum and randomly sample one query per target graph. We lower bound the number of iterations per epoch to 64 for datasets that are too small. For the E-R dataset, where we generate neighborhoods at random, and the WN dataset which consists of only a single graph, we use a fixed 64 iterations per epoch. On all datasets except for the E-R dataset, we used 256 target graphs where possible. At training time, we enforce a 3:1 negative to positive ratio in the training examples, which is necessary since in reality there is a heavy skew in the dataset towards negative examples. 10% of the negative examples are hard negatives; among the remaining 90%, half are negative examples drawn from the same target graph as the query, and half are negative examples drawn from different target graphs.

The model is trained with a learning rate of 1×10^{-3} using the Adam optimizer. The learning rate is annealed with a cosine annealer with restarts every 100 epochs. The curriculum starts with 1 target graph with a radius of 1; it is updated every time there are 20 consecutive epochs without an improvement of more than 0.1. The curriculum update increases the radius of the target graphs by 1 up to a maximum of 4, after which it doubles the number of target graphs for every update up to a maximum of 256. The dataset is regenerated every 50 epochs.

	Predicted +	Predicted -
Positive	68.2	8.3
Negative	70.5	1030.9

Table 6: Average confusion Matrix for matching small queries (size ≤ 7) to all node neighborhoods in the DD dataset.

Hyperparameters. We performed a comprehensive sweep over hyperparameters used in the model. Table 5 shows the effect of hyperparameters and GNN models on the performance, using the NeuroMatch framework. We list the design choices we made that are observed to perform well in both synthetic and real-world datasets:

- Sum aggregation usually works the best, confirming previous theoretical studies [32]. Both the GraphSAGE and GIN architecture we implemented uses the sum neighborhood aggregation.
- We observe slight improvement in performance when using LeakyReLU instead of ReLU for non-linearity.
- Dropout does not have a significant impact on performance.

Dataset	E-R	COX2	DD	MSRC_21	FIRSTMMDB
NO CURR	92.8 ± 0.4	83.4 ± 3.0	82.0 ± 4.3	82.5 ± 5.9	87.5 ± 4.9
NM-MLP	94.1 ± 0.3	87.3 ± 3.2	85.7 ± 3.4	79.8 ± 1.4	92.4 ± 6.6
NM-NTN	94.7 ± 0.8	80.1 ± 2.8	85.3 ± 2.6	79.6 ± 3.1	85.2 ± 3.1
NM-BOX	88.5 ± 1.1	79.4 ± 3.5	77.0 ± 4.5	72.1 ± 2.9	88.9 ± 4.2
NEUROMATCH	94.2 ± 0.4	88.5 ± 2.4	84.5 ± 2.9	83.3 ± 2.1	92.8 ± 4.1

Table 7: Given G_Q for every $q \in G_Q$ we aim to find a matching node $u \in G_T$. The AUROC (unit: 0.01). GMNN and RDGCN do not apply here since they cannot match query nodes to a subset of nodes in the target.

Dataset	ENZYMES	COX2	AIDS	PPI	IMDB-BINARY
TRANSFER	78.9	93.9	92.2	81.0	74.2
IN-DOMAIN	92.9	97.2	94.3	89.9	81.8

Table 8: The AUROC (unit: 0.01) for matching on real datasets, where we either train on the synthetic dataset and test generalization to the real dataset (TRANSFER), or train directly on the dataset that we test on (IN-DOMAIN).

- Adding structural features, such as node degree, clustering coefficient, and average path length improves the convergence speed.

G. Subgraph Matching Results

Label imbalance. We performed additional experiments to investigate the confusion matrix for the DD dataset averaged across test queries. Table 6 shows extreme imbalance (subgraphs are rare). Our threshold results in 12% false negative rate and 50.8% false positive rate.

Identifying all pairs of matching nodes. We further provide comparative studies on the task of matching all nodes (experiment 3), as shown in Table 7. Here a similar trend of the performance of NeuroMatch and its alternatives are observed.

H. Generalization and Runtime

H.1. Pretraining on synthetic dataset

To demonstrate the use and generalizability of the synthetic dataset, we also conduct the experiment where the subgraph matching model is trained only on the synthetic dataset, and is then tested on real-world datasets. Table 8 shows that although there is a drop in performance when the model only sees the synthetic dataset, the model is able generalize to a diverse setting of subgraph matching scenarios, in biology, chemistry and social network domains, even out-performing some baseline methods that are specifically trained on the real-world datasets. However, a shortcoming is that since the synthetic dataset does not contain node features, and real datasets have varying node feature dimensions, the model is only able to consider subgraph matching task that does not take feature into account. Incorporation of feature in transfer learning of subgraph matching remains to be an open problem.

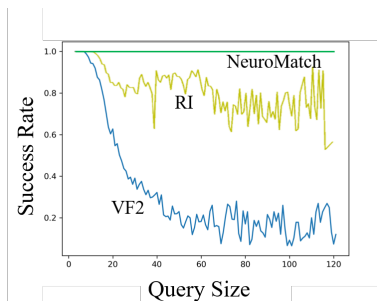


Figure 4: Runtime analysis. Success rate of baseline heuristic matching algorithms (VF2 and RI) for matching in under 20 seconds. NeuroMatch achieves 100% success rate.

We show in Figure 4 the success rate of the baselines, which drop below 60% when the query size is increased to more than 50. In comparison, NeuroMatch always finishes under 0.1 second.

Moreover, since in practice, it is feasible to pre-train the NeuroMatch model on synthetic datasets, and optionally finetune few epochs on real-world datasets, the training time for model when given a new dataset is also negligible. However, such approach has the limitation that the model cannot account for node categorical features when performing subgraph matching, since the synthetic dataset does not contain any node feature.